

Automatic Fuzzy Control Design for Parallel DC-DC Converters

Rong-Jong Wai, MEMBER, IAENG, and Yi-Chang Chen

Abstract—This study mainly focuses on the development of an automatic fuzzy control (AFC) system for a parallel dc-dc converter, and the control objective is to achieve the stable voltage regulation and uniform current distribution. The average model for an example of a three-module boost converter, which is composed of three conventional boost converter frames in parallel connection, is derived for the design of this AFC system including voltage and current control loops. In the voltage control loop, the target of the inductor current is designed to be followed by the current control loop, and the current control loop is designed via incremental fuzzy form to control respective duty ratios. In this AFC scheme, the fuzzy inference mechanism is automatically built according to inherent circuit properties without complex tuning algorithms or computation processes. The effectiveness of the proposed control scheme is verified by numerical simulations, and the advantages of good transient response and robustness to uncertainties are indicated in comparison with a conventional proportional-integral control (PIC) system.

Index Terms—Automatic fuzzy control, Stable voltage regulation, Uniform current distribution, Parallel dc-dc converter, Boost converter.

I. INTRODUCTION

Nowadays, parallel dc-dc converters with fundamental boost mechanism and large power capacity have been widely used in many industrial applications for promoting the level of low-voltage-type sources and satisfying ever demanding power requirements [1]–[3]. With this arrangement, it offers efficient processing of built-in redundancy and ensures the supply of high output currents in applications such as mainframe computers, systems using very large scale integration (VLSI) technology, and uninterruptible power supplies (UPS) [3]. Control of the fundamental boost converter frame in parallel dc-dc converters is a challenging problem because, besides being a bilinear system (with a binary input in its exact description, or a saturated one in the average model) it is also a non-minimum phase system with respect to the output to be controlled [4], [5]. The existence of unstable zero dynamics introduces a hard constraints on the achievable performance [5]. Being a nonlinear system, a parallel-connected system of boost converters may behave in many ways that could not be manipulated by conventional linear design and analytic methods. In order to improve system reliability and reducing current stress on switching devices, the control objective must ensure the

equal sharing of the load current among parallel converters and the stable regulation of the output voltage [3].

Traditionally, conventional proportional-integral-derivative (PID)-type controllers are widely used in industry due to their simple control structure, ease of design, and inexpensive cost [6]. However, the stability of the PID-type control system could not be assured when system uncertainties exist, and the control gain should be repeatedly tuned to ensure favorable performances. Besides, the unbalanced equivalent series resistors (ESR) on inductors of the parallel dc-dc converter would cause the current distribution to be not uniform. To deal with this difficult problem, much research has been done in recent years to apply various approaches in the control field [1]–[3], [7]. Choi [1] investigated three different paralleling schemes for multi-module converters and addressed benefits and limitations for each paralleling scheme. However, the control gain should be predetermined via off-line frequency spectrum analyses with a tradeoff between the current sharing and steady-state voltage error. López *et al.* [3] presented the analysis and design of a parallel-connected converter system using sliding-mode control techniques. But, the local stability of the sliding-mode control system in [3] only could be guaranteed under specific conditions. Mazumder [7] developed analytic methodologies for stability analyses of parallel dc-dc converters using their switching model, discrete model and average model. Unfortunately, only the methodology using a load-sharing dc-dc buck converter was illustrated.

Fuzzy control (FC) using linguistic information possesses several advantages such as robustness, model-free, universal approximation theorem and rule-based algorithm [8], [9]. In this study, an automatic fuzzy control (AFC) system is designed for a parallel dc-dc converter to simultaneously achieve the stable voltage regulation and uniform current distribution. This study is organized into five sections. Following the introduction, the entire three-module boost converter structure and its dynamic average model are briefly described in Section II. Moreover, the detailed design procedure of the AFC system are explained in Section III. In Section IV, comparative simulations with proportional integral control (PIC) for a three-module boost converter are performed to demonstrate the effectiveness and robust control performance of the proposed AFC scheme. Finally, some conclusions are drawn in Section V.

II. SYSTEM DESCRIPTION

In this study, a three-module boost converter is composed of three conventional boost converter frames in parallel connection and its configuration is depicted in Fig.

Manuscript received July 21, 2008. This work was supported in part by the National Science Council of Taiwan, R.O.C. through grant number NSC 97-2221-E-155-065-MY2.

The authors are with the Department of Electrical Engineering, Yuan Ze University, Chung Li, Taiwan 32003, R.O.C. (phone: 886-3-4638800 ext 7117; fax: 886-3-4639355; e-mail: rjwai@saturn.yzu.edu.tw).

1. In this converter, it uses a common input voltage source (v_i), and the corresponding input current (i_i) distributes over three basic converter frames. The major symbol representations are summarized as follows. In Fig. 1, v_i denotes a dc input voltage; $i_{L_n}|_{n=1,2,3}$ and $r_{L_n}|_{n=1,2,3}$ are the currents and equivalent series resistors (ESR) of respective inductors $L_n|_{n=1,2,3}$. Moreover, $S_n|_{n=1,2,3}$ and $D_n|_{n=1,2,3}$ represent the switches and output rectifier diodes; C is the output filter capacitor and R is the output load; i_o and v_o are the output current and voltage. Note that, the conductive voltage drops of all the switches $S_n|_{n=1,2,3}$ and diodes $D_n|_{n=1,2,3}$ are neglected in this study to simplify circuit analyses. In addition, the current source i_u imitates system uncertainties incurred by the load variations, the effect of ESR in the output filter capacitor, ideal assumptions in circuit analyses, and unpredictable perturbations in practical applications.

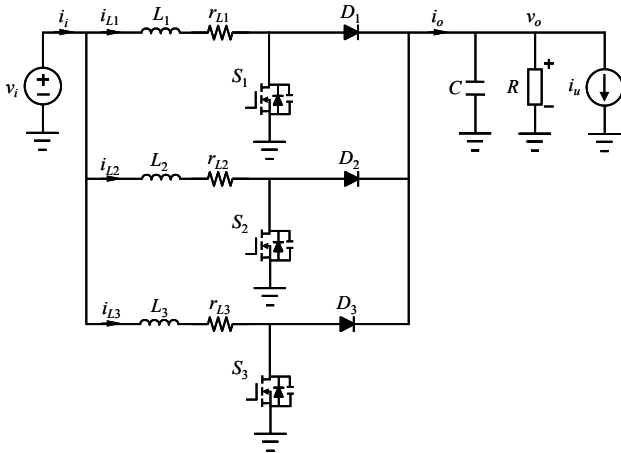


Fig. 1. Framework of three-module boost converter.

Apply nodal and loop analytic techniques [10], the dynamic behavior of this three-module boost converter can be governed by the following state equations:

$$\frac{di_{L1}}{dt} = \frac{-(1-v_1)v_o}{L_1} + \frac{v_i}{L_1} - \frac{i_{L1}r_{L1}}{L_1} \quad (1)$$

$$\frac{di_{L2}}{dt} = \frac{-(1-v_2)v_o}{L_2} + \frac{v_i}{L_2} - \frac{i_{L2}r_{L2}}{L_2} \quad (2)$$

$$\frac{di_{L3}}{dt} = \frac{-(1-v_3)v_o}{L_3} + \frac{v_i}{L_3} - \frac{i_{L3}r_{L3}}{L_3} \quad (3)$$

$$\frac{dv_o}{dt} = \frac{-v_o}{L_2} + \frac{i_u}{C} - \frac{i_o}{C} \quad (4)$$

where $v_n|_{n=1,2,3}$ denote the states of the switches $S_n|_{n=1,2,3}$. When $v_n = 1$, it means that the switch S_n is turned on. Similarly, if the switch S_n is turned off, then $v_n = 0$. According to (1)–(4), the average model of this three-module boost converter can be derived via the state-space averaging method [10] as

$$L_1 \dot{z}_1 + r_{L1} z_1 - v_i = (u_1 - 1) z_4 \quad (5)$$

$$L_2 \dot{z}_2 + r_{L2} z_2 - v_i = (u_2 - 1) z_4 \quad (6)$$

$$L_3 \dot{z}_3 + r_{L3} z_3 - v_i = (u_3 - 1) z_4 \quad (7)$$

$$C \dot{z}_4 + \frac{1}{R} z_4 + (z_u - z_o) = 0 \quad (8)$$

where z_1, z_2, z_3, z_4, z_o and z are the average values of $i_{L1}, i_{L2}, i_{L3}, v_o, i_o$ and i_u , respectively; the control input $u_n|_{n=1,2,3}$ denote respective duty ratios of the switches $S_n|_{n=1,2,3}$.

III. AUTOMATIC FUZZY CONTROL

The block diagram of an automatic fuzzy control (AFC) system including voltage and current control loops for the three-module boost converter is depicted in Fig. 2, where z_{4d} is the voltage command and z_{cd} is the total amount of inductor current commands specified by the voltage control loop. By dividing z_{cd} equally to force uniform current distribution (i.e., $n_i = 3$), z_{1d}, z_{2d} and z_{3d} represent respective inductor current commands. The control problem is to find a suitable control law so that the output voltage z_4 can track a desired reference command z_{4d} and the inductor currents can achieve uniform current distribution. To achieve this control objective, define a voltage tracking error $e_v = z_{4d} - z_4$ and three inductor current tracking errors, $e_n|_{n=1,2,3} = z_{nd}|_{n=1,2,3} - z_n|_{n=1,2,3}$. The detailed derivations of the proposed AFC system including voltage and current control loops are described in the following subsections.

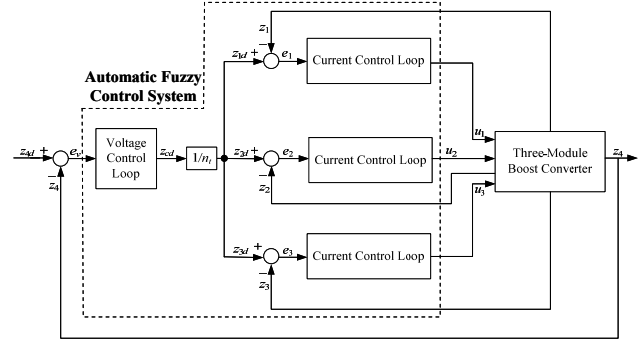


Fig. 2. Block diagram of automatic fuzzy control system.

A. Voltage Control Loop

The input linguistic variables for this fuzzy voltage control are the voltage tracking error $e_v(n_i)$ and its change rate $e'_v(n_i)$, which are defined as

$$e_v(n_i) \triangleq z_{4d}(n_i) - z_4(n_i) \quad (9)$$

$$e'_v(n_i) \triangleq [e_v(n_i) - e_v(n_i - 1)] / t_s \quad (10)$$

where n_i is the number of iterations; t_s is the sampling time, $z_{4d}(n_i)$ is the voltage command at n_i -th sampling interval; $z_4(n_i)$ the output voltage at n_i -th sampling

interval; $e_v(n_i)$ is the voltage tracking error at n_i -th sampling interval; $e'_v(n_i)$ is the change rate of voltage tracking error at n_i -th sampling interval. Moreover, the output linguistic variable is the increment of the total inductor current command, $\Delta z_{cd}(n_i)$. In this study, the entire inductor current command in the fuzzy voltage control can be expressed as

$$z_{cd} = \Delta z_{cd} + [(P_{\max} / \bar{v}_i) / 2] \quad (11)$$

where \bar{v}_i is the nominal input voltage; P_{\max} is the predetermined maximum input power, and the term $[(P_{\max} / \bar{v}_i) / 2]$ in (11) represents the base of the total inductor current command. In addition, the input and output fuzzy sets are both chosen as Positive Big (PB), Positive Small (PS), Zero (ZE), Negative Small (NS), and Negative Big (NB). The membership functions of input and output fuzzy sets in the voltage control loop are depicted in Figs. 3 and 4, respectively. In this study, the singleton fuzzification with triangular membership functions, center-of-gravity defuzzification, and product fuzzy inference are adopted because they are computationally simple, intuitively plausible, and most frequently used in the opening literatures [8], [9].

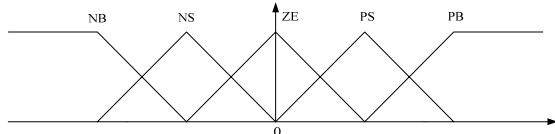


Fig. 3. Membership functions of input fuzzy sets.

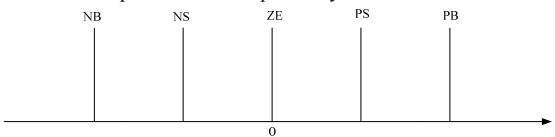


Fig. 4. Membership functions of output fuzzy sets.

Fuzzy control is characterized by a collection of fuzzy IF-THEN rules, in which the preconditions and consequents involve linguistic variables. The rule base in the fuzzy voltage control can be represented as

$$R^l: \text{If } e_v(n_i) \text{ is } F_1^l \text{ and } e'_v(n_i) \text{ is } F_2^l, \quad (12)$$

Then $\Delta z_{cd}(n_i)$ is g^l

where F_1^l and F_2^l are input fuzzy sets; g^l is the output fuzzy set (singleton action); $l = 1, \dots, m_v$, where m_v is the number of rules in the voltage control loop. According to inherent circuit properties, the total inductor current command should be increased if both the voltage tracking error and its change rate are positive. On the contrary, the total inductor current command should be decreased if both the voltage tracking error and its change rate are negative. From these analyses, fuzzy linguistic rules used in the voltage control loop can be summarized in Table I. As a result, the increment of the total inductor current command produced by the fuzzy voltage control can be expressed as

$$\Delta z_{cd} = \sum_{l=1}^{m_v} w_l r_l / \sum_{l=1}^{m_v} w_l \quad (13)$$

where r_l is the singleton of the output fuzzy set, and w_l is the firing strength of the corresponding rule.

B. Current Control Loop

The input linguistic variables for the fuzzy current control are current tracking errors $e_n(n_i)|_{n=1,2,3}$ and their change rates $e'_n(n_i)|_{n=1,2,3}$, which are defined as

$$e_n(n_i)|_{n=1,2,3} \triangleq z_{nd}(n_i)|_{n=1,2,3} - z_n(n_i)|_{n=1,2,3} \quad (14)$$

$$e'_n(n_i)|_{n=1,2,3} \triangleq [e_n(n_i)|_{n=1,2,3} - e_n(n_i-1)|_{n=1,2,3}] / t_s \quad (15)$$

where $z_{nd}(n_i)|_{n=1,2,3}$ are respective inductor current commands at n_i -th sampling interval; $z_n(n_i)|_{n=1,2,3}$ are respective inductor currents at n_i -th sampling interval; $e_n(n_i)|_{n=1,2,3}$ are respective current tracking errors at n_i -th sampling interval; $e'_n(n_i)|_{n=1,2,3}$ are the change rates of respective current tracking errors at n_i -th sampling interval. Moreover, the output linguistic variables are respective incremental duty ratios, $\Delta u_n(n_i)|_{n=1,2,3}$. In this study, the entire duty ratios in the fuzzy current control can be expressed as

$$u_n|_{n=1,2,3} = \Delta u_n|_{n=1,2,3} + (1 - \bar{v}_i / z_{4d}) \quad (16)$$

where the term $(1 - \bar{v}_i / z_{4d})$ represents the nominal duty ratio of a conventional boost converter. In addition, the input and output fuzzy sets of the fuzzy current control are chosen as the same as the ones of the fuzzy voltage control. The membership functions of input and output fuzzy sets in the current control loop are also depicted in Figs. 3 and 4, respectively. The singleton fuzzification with triangular membership functions, center-of-gravity defuzzification, and product fuzzy inference [8], [9] are also adopted here. The rule base in the fuzzy current control can be represented as

$$R^j: \text{If } e_n(n_i)|_{n=1,2,3} \text{ is } F_1^j \text{ and } e'_n(n_i)|_{n=1,2,3} \text{ is } F_2^j, \quad (17)$$

Then $\Delta u_n(n_i)|_{n=1,2,3}$ is g^j

where F_1^j and F_2^j are input fuzzy sets; g^j is the output fuzzy set (singleton action); $j = 1, \dots, m_c$, where m_c is the number of rules in the current control loop.

TABLE I.
FUZZY LINGUISTIC RULES

Error change rate \ Error	PB	PS	ZE	NS	NB
PB	PB	PB	PB	PS	ZE
PS	PB	PB	PS	ZE	NS
ZE	PB	PS	ZE	NS	NB
NS	PS	ZE	NS	NB	NB
NB	ZE	NS	NB	NB	NB

According to inherent circuit properties, the duty ratio should be increased (i.e., charge the inductor more time) if both the current tracking error and its change rate are positive. On the contrary, the duty ratio should be decreased (i.e., discharge the inductor more time) if both the current tracking error and its change rate are negative. From these analyses, fuzzy linguistic rules in Table I also can be used in the current control loop. As a result, the incremental duty ratio $\Delta u_n|_{n=1,2,3}$ produced by the fuzzy

current control can be expressed as

$$\Delta u_n = \sum_{j=1}^m w_j^n r_j^n / \sum_{j=1}^m w_j^n, \quad n = 1, 2, 3 \quad (18)$$

where r_j^n is the singleton of the output fuzzy set, and w_j^n is the firing strength of the corresponding rule.

IV. NUMERICAL SIMULATIONS

In order to exhibit the merits of the proposed automatic fuzzy control (AFC) system, a conventional proportional-integral control (PIC) system is also examined in this study [6]. In this PIC scheme, the voltage tracking error e_v is obtained by subtracting z_4 from z_{4d} , and the total amount of inductor current commands is designed as $z_{cd} = k_{p1}e_v + k_{i1} \int_0^t e_v dt$, in which k_{p1} and k_{i1} are proportional and integral gains in the voltage control loop. Then, z_{cd} is divided equally to z_{1d} , z_{2d} and z_{3d} (i.e., $n_i = 3$) for viewing as respective inductor current commands, and the corresponding current tracking errors $e_n|_{n=1,2,3} = z_{nd}|_{n=1,2,3} - z_n|_{n=1,2,3}$ are used to design the control efforts as $u_n|_{n=1,2,3} = k_{p2}e_n|_{n=1,2,3} + (1 - \bar{v}_i / z_{4d})$, in which k_{p2} is a proportional gain in the current control loop. Moreover, assume that input fuzzy sets in the proposed AFC system are symmetrical, the center (c_r^h) and width (w_d) of triangular membership functions can be determined by dividing equally as

$$c_r^h|_{h=1, \dots, n_f} = x_{\max} - (h-1) \frac{x_{\max} - x_{\min}}{n_f - 1} \quad (19)$$

$$w_d = 2 \frac{x_{\max} - x_{\min}}{n_f - 1} \quad (20)$$

where n_f is the total number of input/output fuzzy sets; x_{\max} and x_{\min} could be predetermined maximal and minimal bounds of e_v , e'_v , Δz_{cd} , $e_n|_{n=1,2,3}$, $e'_n|_{n=1,2,3}$ and

$$\Delta u_n|_{n=1,2,3}.$$

All numerical simulations are carried out using Windows packaged Matlab 6.5 edition software. The circuit specifications of a three-module boost converter with nominal output power $P_o = 400$ W are summarized as follows:

PWM switching frequency	$f_s = 20$ kHz ;
Sampling time	$T = 50$ μ s ;
Inductors	$L_1 = 560$ μ H ; $L_2 = 565$ μ H ; $L_3 = 584$ μ H ;
Output filter capacitor	$C = 13.2$ mF ;
Rated output load	$R = 5.76$ Ω ;
Nominal input voltage	$\bar{v}_i = 24$ V ;
Nominal voltage command	$z_{4d} = 48$ V .

Moreover, the initial conditions are set at $z_1(0) = z_2(0) = z_3(0) = 1.3889$ A and $z_4(0) = 24$ V . In

addition, the control parameters of PIC and AFC systems are given as

$$n_i = 3, \quad n_f = 5, \quad m_v = m_c = 25, \quad k_{p1} = 3, \quad k_{i1} = 5000, \quad k_{p2} = 0.045 \quad (21)$$

All the parameters in (21) are chosen to achieve superior transient control performance in numerical simulations by considering the possible occurrence of operational conditions and the limitation of control efforts.

In order to investigate the robust characteristics of the proposed AFC system, the following examined cases are considered:

Case 1: Robustness against load variations.

$v_i = 24$ V ; $r_{L1} = r_{L2} = r_{L3} = 0$; R is changed from 5.76Ω to 4.189Ω at $t=0.15$ sec and then from 4.189Ω to 9.216Ω at $t=0.30$ sec.

Case 2: Robustness against load variations and different equivalent series resistors of inductors.

$v_i = 24$ V ; $r_{L1} = 56$ m Ω ; $r_{L2} = 56.5$ m Ω ; $r_{L3} = 78.4$ m Ω ; R is changed from 5.76Ω to 4.189Ω at $t=0.15$ sec and then from 4.189Ω to 9.216Ω at $t=0.30$ sec.

Case 3: Robustness under the occurrence of i_u .

$v_i = 24$ V ; $r_{L1} = r_{L2} = r_{L3} = 0$; $i_u = 2 \sin(377t)$; $R = 5.76 \Omega$

Case 4: Robustness against load variations and different voltage commands.

$v_i = 24$ V ; $r_{L1} = r_{L2} = r_{L3} = 0$; R is changed from 5.76Ω to 4.189Ω at $t=0.15$ sec and then from 4.189Ω to 9.216Ω at $t=0.30$ sec; z_{4d} is changed from 48 V to 55 V at $t=0.20$ sec.

All the illustrations of the PIC and AFC systems are depicted in Figs. 5–12. The sub-figure (a) is the voltage tracking response; the sub-figure (b) is the inductor current distribution; the sub-figure (c) is the corresponding voltage tracking error; the sub-figure (d) is the corresponding current tracking errors.

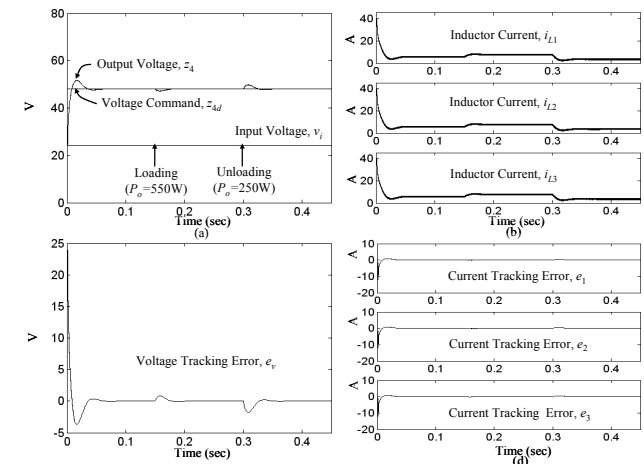


Fig. 5. Numerical simulations of PIC system for three-module boost converter at case 1: (a) Voltage tracking response; (b) Inductor current distribution; (c) Voltage tracking error; (d) Current tracking error.

Numerical simulations of the PIC system for the

three-module boost converter at cases 1–4 are depicted in Figs. 5–8, respectively. From Fig. 5(a), one can see that the output voltage at cases 1 show a little bit dip and a slight overshoot while load variation but is eventually restored to its desired value. Basically, the average current distribution is uniform in this incremental-type PIC scheme. As can be seen from Fig. 6(a), the output voltage at case 2 also shows a slight dip while loading and a slight overshoot while unloading but rapidly restored to its desired value. At case 3, the output voltage ripple in Fig. 7(a) is distinct because the inductor current is not large enough to compensate the effect of i_u . From Fig. 8(a), the output voltage at case 4 shows a little bit dip and a slight overshoot under load variation and voltage command change. Besides, the average current distribution in Figs. 6(b) and 8(b) is not very uniform because of the difference of $r_{Lj} |_{j=1,2,3}$ and voltage commands.

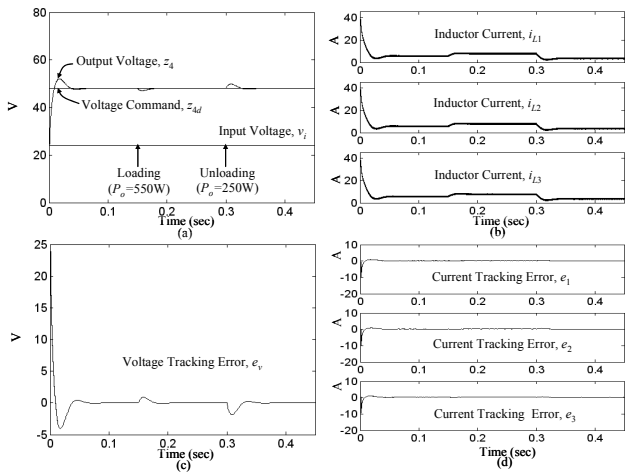


Fig. 6. Numerical simulations of PIC system for three-module boost converter at case 2: (a) Voltage tracking response; (b) Inductor current distribution; (c) Voltage tracking error; (d) Current tracking error.

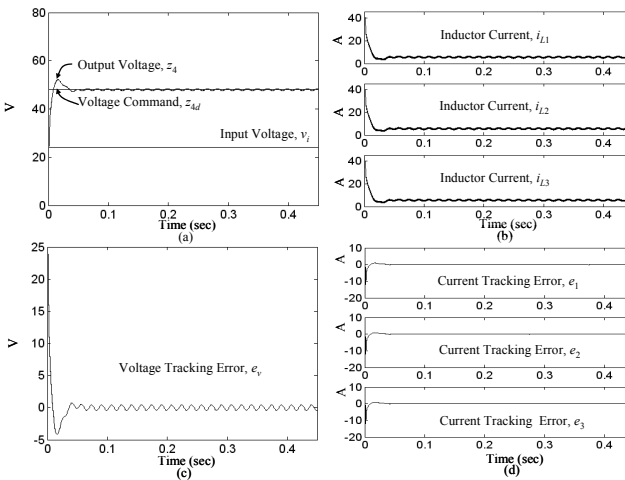


Fig. 7. Numerical simulations of PIC system for three-module boost converter at case 3: (a) Voltage tracking response; (b) Inductor current distribution; (c) Voltage tracking error; (d) Current tracking error.

For comparison, numerical simulations of the proposed AFC system for the three-module boost converter at cases 1–4 are provided in Figs. 9–12, respectively. The control

performances at cases 1, 2 and 4 are quite stable and insensitive to the load variations or to the occurrence of different equivalent inductor series resistors and voltage commands. In other words, the output voltage rapidly stabilizes without any voltage drop or overshoot, and the average inductor current distribution is uniform. At case 3, the output voltage ripple in Fig. 7(a) can be greatly improved by the proposed AFC system, and the uniform current distribution also can be achieved. Compare Figs. 9–12 with Figs. 5–8, the proposed AFC system indeed yields superior performance than the PIC system.

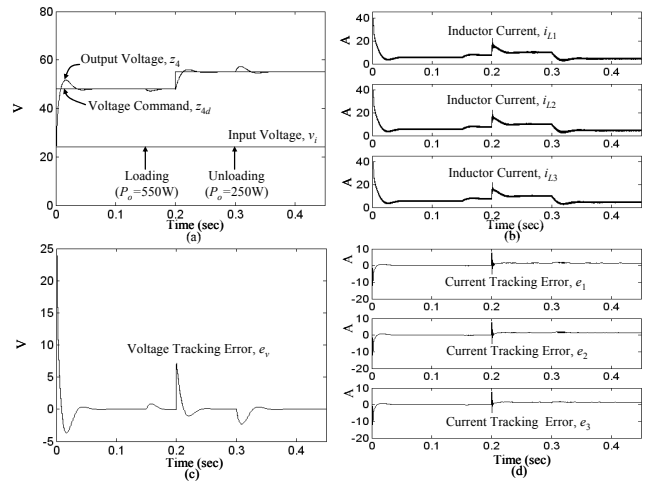


Fig. 8. Numerical simulations of PIC system for three-module boost converter at case 4: (a) Voltage tracking response; (b) Inductor current distribution; (c) Voltage tracking error; (d) Current tracking error.

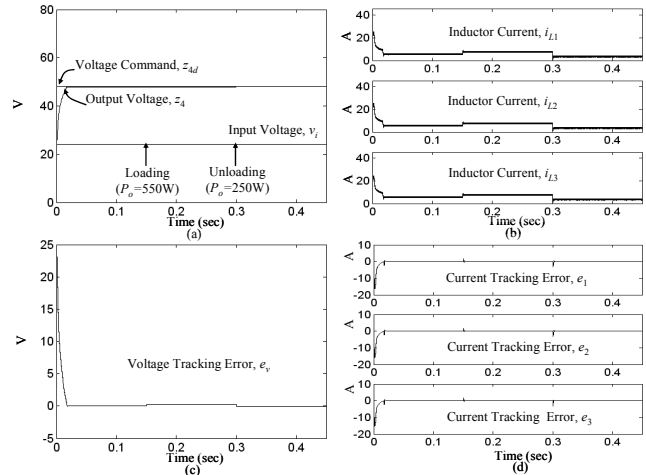


Fig. 9. Numerical simulations of AFC system for three-module boost converter at case 1: (a) Voltage tracking response; (b) Inductor current distribution; (c) Voltage tracking error; (d) Current tracking error.

V. CONCLUSIONS

This study has successfully developed an automatic fuzzy control (AFC) system with inherent circuit property design for the stable voltage regulation and uniform current distribution of a parallel dc-dc converter. Numerical simulations are presented to illustrate the effectiveness of the proposed AFC scheme for a three-module boost converter, and the merits are indicated in comparison with a conventional proportional-integral control (PIC) system.

According to the simulated results, one can see that the voltage regulation ability is excellent and the current sharing is very uniform even if under the possible occurrence of system uncertainties. Consequently, the proposed AFC scheme is more suitable for the parallel dc-dc converter than the traditional PIC system.

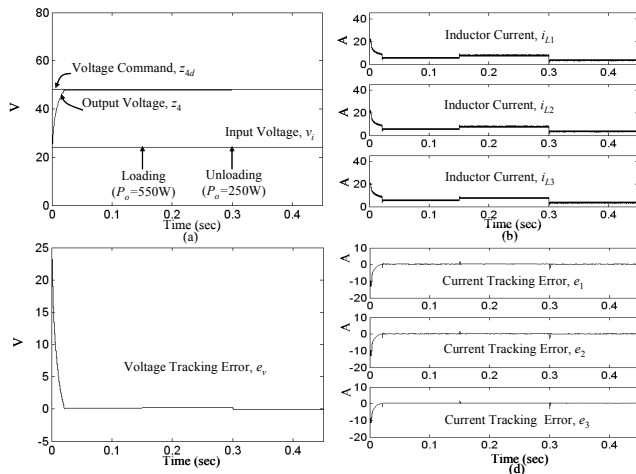


Fig. 10. Numerical simulations of AFC system for three-module boost converter at case 2: (a) Voltage tracking response; (b) Inductor current distribution; (c) Voltage tracking error; (d) Current tracking error.

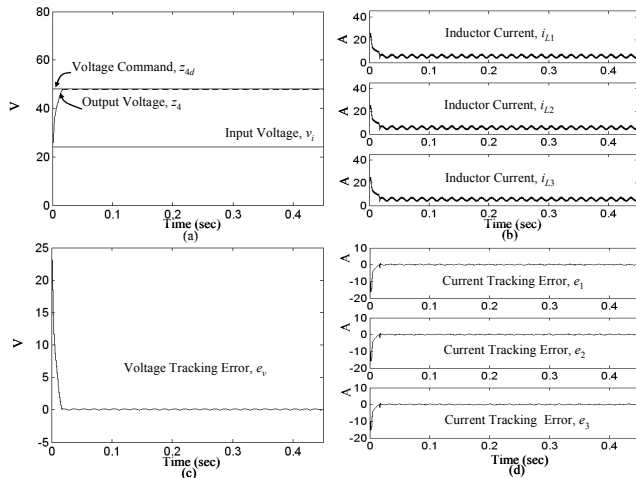


Fig. 11. Numerical simulations of AFC system for three-module boost converter at case 3: (a) Voltage tracking response; (b) Inductor current distribution; (c) Voltage tracking error; (d) Current tracking error.

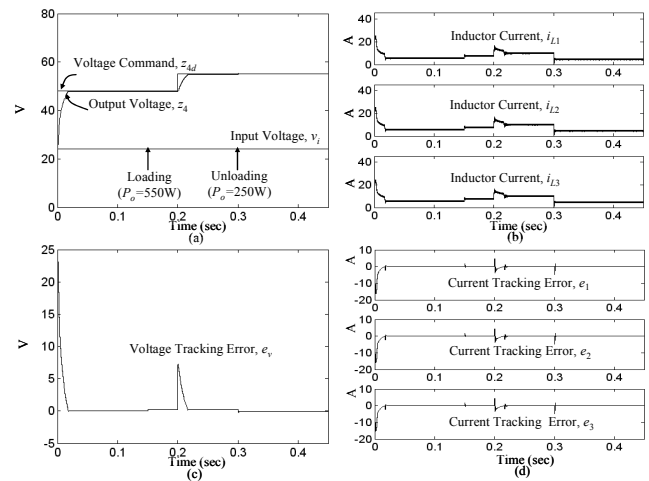


Fig. 12. Numerical simulations of AFC system for three-module boost converter at case 4: (a) Voltage tracking response; (b) Inductor current distribution; (c) Voltage tracking error; (d) Current tracking error.

REFERENCES

- [1] B. Choi, "Comparative study on paralleling schemes of converter modules for distributed power applications," *IEEE Trans. Ind. Electron.*, vol. 45, no. 2, pp. 194-199, 1998.
- [2] H. H. C. Ju and C. K. Tse, "Study of low-frequency bifurcation phenomena of a parallel-connected boost converter system via simple averaged models," *IEEE Trans. Circuits Syst. I*, vol. 50, no. 5, pp. 679-686, 2003.
- [3] M. López, L. G. de Vicuña, M. Castilla, P. Gayà, and O. López, "Current distribution control design for paralleled DC/DC converters using sliding-mode control," *IEEE Trans. Ind. Electron.*, vol. 51, no. 2, pp. 419-428, 2004.
- [4] H. Sira-Ramirez, R. A. Perez-Moreno, R. Ortega, and M. Garcia-Esteban, "Passivity-based controllers for the stabilization of DC-to-DC power converters," *Automatica*, vol. 33, no. 4, pp. 499-513, 1997.
- [5] G. Escobar, R. Ortega, H. Sira-Ramirez, J. P. Vilain, and I. Zein, "An experimental comparison of several nonlinear controllers for power converters," *IEEE Control System Magazine*, vol. 19, no. 1, pp. 66-82, 1999.
- [6] K. J. Astrom and T. Hagglund, *PID Controller: Theory, Design and Tuning*. Research Triangle Park, NC: ISA, 1995.
- [7] S. K. Mazumder, "Stability analysis of parallel DC-DC converters," *IEEE Trans. Aero. Electron. Syst.*, vol. 42, no. 1, pp. 50-69, 2006.
- [8] L. X. Wang, *Adaptive Fuzzy Systems and Control: Design and Stability Analysis*. New Jersey: Prentice-Hall, 1994.
- [9] J. R. Timothy, *Fuzzy Logic with Engineering Application*. New York: McGraw-Hill, 1995.
- [10] N. Mohan, T. M. Undeland, and W. P. Robbins, *Power Electronics: Converters, Applications, and Design*. New York: John Wiley & Sons, 1995.